

Online: ISSN 2008-949X

Journal of Mathematics and Computer Science



Journal Homepage: www.isr-publications.com/jmcs

A new spectral framework for solving fractional-order differential equations: improved efficiency without residual functions



Danish Zaidi^a, Imran Talib^b, Muhammad Bilal Riaz^{a,c,d,*}

Abstract

The Spectral Tau method is a widely recognized numerical technique employed for solving fractional-order differential equations (FODEs). The central focus of the Spectral Tau method's algorithm depends on the idea of operational matrices derived from the basis sets of orthogonal polynomials, which are utilized to approximate derivative terms in the problems. In this study, our main objective is to introduce a new numerical method within the class of spectral methods, but distinct in its formulation from the Spectral Tau method. While both approaches utilize operational matrices of orthogonal polynomials, the proposed method avoids the computation of residual functions, which is a key step in the Spectral Tau method. Another important feature of the proposed study is the construction of novel generalized integral operational matrices in the Riemann-Liouville sense, developed using a basis of orthogonal shifted Laguerre polynomials (OSLPs). This structure leads to simplified implementation, reduced computational cost, and enhanced spectral accuracy. To demonstrate the efficiency and practical applicability of the proposed method, we solve several test problems. Additionally, we compare the computational efficiency and the absolute errors obtained using our proposed method with those derived from the Spectral Tau method.

Keywords: Generalized fractional-order operators, generalized operational matrices, orthogonal polynomials, Sylvester equations, Laguerre polynomials, spectral methods.

2020 MSC: 65L60, 65N35, 65M70, 26A33.

©2026 All rights reserved.

1. Introduction

Fractional calculus was conceived as a result of a philosophical discussion that took place on September 30, 1695, between two of the most well-known mathematicians of all time, L'Hospital and Leibniz. For a long period, it was perceived as a mathematical curiosity having no relevance to the physical sciences or any other fields associated with the scientific study of nature. The first significant use of fractional operators was reportedly by Abel, who solved the "Tautochrone problem" which involves determining the curve on which a particle, starting from any initial position and moving without friction, takes the same amount

*Corresponding authors

Email address: muhammad.bilal.riaz@vsb.cz (Muhammad Bilal Riaz)

doi: 10.22436/jmcs.041.02.05

Received: 2025-05-23 Revised: 2025-06-28 Accepted: 2025-07-28

^aDepartment of Mathematics, University of Management and Technology, 54770 Lahore, Pakistan.

^bDepartment of Mathematics, Nonlinear Analysis Group (NAG), Virtual University of Pakistan, 54-Lawrence Road, Lahore, Pakistan.

^cIT4Innovations, VSB-Technical University of Ostrava, Ostrava, Czech Republic.

^dApplied Science Research Center, Applied Science Private University, Amman, Jordan.

of time to reach the bottom, regardless of its starting point. This challenge was resolved in 1823. Initially foreseen by Leibniz as a potential paradox, the subject has since developed significantly, attracting the attention of numerous researchers across diverse engineering and scientific fields ([8, 10, 26, 29]).

Among the widely used numerical techniques for addressing fractional order differential equations (FODEs) are spectral methods and finite difference methods. However, finite-difference techniques have certain limitations, such as linear convergence and applicability only to commensurate-order FODEs. In contrast, spectral methods have been effectively applied to both commensurate-order and incommensurate-order FODEs. These methods use operational matrices of derivatives, integrals, or both, associated with orthogonal polynomials, to convert FODEs into algebraic equations that can be easily solved. As a result, spectral methods offer exponential convergence, providing more accurate solutions compared to finite difference methods.

A considerable amount of research articles exist in the literature where researchers have solved FODEs using spectral methods, the construction of which primarily depends on the operational matrices of orthogonal polynomials. As an example, in [27], the fractional-order derivative operational matrix (FODOM) in Caputo sense is derived by using the basis set of shifted Legendre polynomials to approximate the derivative terms in the problem, then the spectral Tau method (STM) is implemented to reduce the linear FODEs into a system of algebraic equations (SAEs). Finally, the solution of the SAEs leads to the solution of the original FODEs. In [4, 5], the FODOM in Caputo setting, based on OSLPs, is constructed, and then the FODEs are reduced to the SAEs using the same approach developed in [27]. The fractional order integral operational matrix (FOIOM) in Riemann-Liouville framework is constructed in [7] with OSLPs to construct the residual function, implementing the STM in order to obtain the SAEs. In [6], a generalized OSLPs basis constructs the FOIOM in Riemann-Liouville setting, with STM applied for reducing FODEs to algebraic form. In [31], the generalized Legendre polynomials have been used to propose the FODOM in Caputo sense and FOIOM in Riemann-Liouville sense for reducing the FODEs into SAEs without implementing the STM and spectral collocation method as proposed in [4-7, 27]. The method presented in [31] is user-friendly and computationally less costly than the methodology followed in [4–7, 27].

Motivated by the studies cited above, we propose a new modified family of spectral methods by incorporating a new modification to the existing spectral methods [4–7, 27, 31]. In these methods, as discussed in [4–7, 27], the spectral Tau and/or spectral collocation methods are used to obtain the corresponding SAEs. The STM, however, requires the computation of residual functions, which can limit its applicability in certain cases due to potential computational difficulties and precision concerns. This is because the high value of the residual indicates a large error in the approximations. Furthermore, solving the SAEs within the STM framework necessitates the use of an appropriate numerical method. On the other hand, the method presented in [31] has the ability of reducing the FODEs into the SAEs without using the STM but needs both FODOM and FOIOM to serve the purpose. That makes it less friendly for users because of the construction of two operational matrices which increased the theoretical work. On the same approach as adopted in [4–7, 27, 31], the structure of our proposed method also depends using operational matrices of orthogonal polynomials. However, unlike traditional approaches, our method does not require the application of the spectral Tau condition or the use of spectral collocation methods to derive the SAEs. Our propose method directly transforms the FODEs into a SAEs. Also, the proposed approach can reduce the FODEs into SAEs having only one operational matrix, named the FOIOM, which is developed in Caputo sense by using the basis set of generalized OSLPs.

The paper is organized as follows. In Section 2, we introduce fractional-order operators and discuss some of their key properties, which are used throughout the work. Section 3 focuses on the properties of generalized OSLPs and provides their analytical formula. In Section 4, we stae and prove the important results that support the construction of operational matrices. Section 5 details the formulation of the numerical method. In Section 6, the accuracy and efficiency of the proposed numerical method (PNM) is demonstrated through the solution of various examples, with the results compared to those obtained using other numerical approaches. The final section summarizes the findings of the study.

2. Preliminaries of fractional calculus

In contrast to conventional derivatives and integrals, fractional order derivatives and integrals do not have a single, unified definition. It has been shown that vmultiple fractional derivative and integral operators, including Caputo, Riemann-Liouville (RL), Atangana-Baleanu (ABC), Hilfer, and Hadamard [2, 13, 20], among others, can be effectively applied to solve a wide range of mathematical problems. Among these, the RL and Caputo operators, which involve fractional integrals, are the most widely studied [18, 20]. The RL fractional-order integral extends the traditional concept of integration to functions with non-integer orders. It is defined as

$$_{RL}J_{\alpha^{+}}^{\delta}u(t)=\frac{1}{\Gamma(\delta)}\int_{\alpha}^{t}(t-x)^{\delta-1}u(x)dx\text{, }t>\alpha\text{, }\delta>0.$$

So, the fractional-order derivatives operators in Riemann-Liouville's sense and Caputo's sense are defined in the follows

$$\begin{split} {}_{RL}\mathcal{D}_{\alpha^{+}}^{\delta}u(t) &= D_{RL}^{n}J_{\alpha^{+}}^{n-\delta}u(t) = \frac{1}{\Gamma(n-\delta)}\frac{d^{n}}{dt^{n}}\int_{\alpha}^{t}(t-x)^{n-\delta-1}u(x)dx, \ t>\alpha, \\ {}_{C}\mathcal{D}_{\alpha^{+}}^{\delta}u(t) &=_{RL}J_{\alpha^{+}}^{n-\delta}D^{n}u(t) \\ &= \frac{1}{\Gamma(n-\delta)}\int_{\alpha}^{t}(t-x)^{n-\delta-1}u^{(n)}(x)dx, \ t>\alpha, \ n-1<\delta< n, \ n\in\mathbb{N}, \ \delta>0, \end{split}$$

where $n-1 < \delta < n$, $n \in \mathbb{N}$, and $\delta > 0$. The Caputo fractional derivative operator is widely used in the fractional modeling of physical phenomena because of its alignment with integer order initial and boundary conditions. In addition, it demonstrates characteristics that are comparable to the derivatives of integer orders. The Caputo operator satisfies the following:

$$_{RL}J_{\alpha^{+}C}^{\delta}\mathcal{D}_{\alpha^{+}}^{\delta}u(t) = u(t) - \sum_{l=0}^{n-1} \frac{u^{(l)}(\alpha)}{l!}(t-\alpha)^{l}, \quad t > \alpha, \quad n-1 < \delta < n, \tag{2.1}$$

and $_{C}\mathcal{D}_{a^{+}}^{\delta}B=0$, where B is constant. The following generalized fractional integral (GFI) operators are constructed by establishing a fractional integral of one function relative to another function ([15, 16, 28]).

Definition 2.1. The GFI operator of order $\delta > 0$ of the function u(t) is defined as

$$_{RL}J_{\alpha^{+}}^{\delta,\eta}u(t)=\frac{\eta^{1-\delta}}{\Gamma(\delta)}\int_{\alpha}^{t}x^{\eta-1}(t^{\eta}-x^{\eta})^{\delta-1}u(x)dx,\quad t>\alpha\geqslant0,\ \eta>0, \tag{2.2}$$

provided that the integral is well defined.

Definition 2.2. The generalized fractional derivative (GFD) operator in RL type of order $\delta > 0$ of the function $\mathfrak{u}(t)$ is defined as

$$_{RL}\mathcal{D}_{\alpha^{+}}^{\delta,\eta}u(t)=\frac{\eta^{\delta-n-1}}{\Gamma(n-\delta)}\bigg(t^{1-\eta}\frac{d}{dt}\bigg)^{n}\int_{0}^{t}x^{\eta-1}(t^{\eta}-x^{\eta})^{n-\delta-1}u(x)dx,\quad t>\alpha\geqslant0,\ \eta>0. \tag{2.3}$$

Definition 2.3. The GFD operator in Caputo sense of order $\delta > 0$ of the function $\mathfrak{u}(t)$ is defined as

$${}_{C}\mathcal{D}_{a^{+}}^{\delta,\eta}u(t) = \frac{\eta^{\delta-n-1}}{\Gamma(n-\delta)} \int_{a}^{t} x^{\eta-1} (t^{\eta} - x^{\eta})^{n-\delta-1} \left(t^{1-\eta} \frac{d}{dt}\right)^{n} u(x), \quad t > a \geqslant 0, \quad \eta > 0,$$
 (2.4)

where $n-1 < \delta < n$.

3. Laguerre polynomials and their characteristics

The French mathematician Edmond Laguerre introduced Laguerre polynomials in the late 19th century, are sets of functions that are mutually perpendicular and have significant importance in mathematical and computational methodologies, including numerical integration, approximation theory, and the resolution of differential equations [30]. Additionally, they established linkages with probability theory, namely in the examination of random variables and stochastic processes. These polynomials are also useful in the analysis of queuing systems and other stochastic models. Their presentation in the radial component for a single electron atom and their characterization of the stationary Wigner functions of oscillator systems in quantum mechanics have significant implications for the field of quantum physics. Laguerre polynomials have been widely employed in solving real problems, including the Lane-Emden equation, Bratu's equation, and Burger's equation [25]. Let $L_k^{(\beta)}(t)$ be the generalized OSLPs of degree k, for $\beta > -1$,

$$L_{k+1}^{(\beta)}(t) = \frac{1}{k+1}[(2k+\beta+1-t)L_k^{\beta}(t) - (k-\beta)L_{k-1}^{\beta}(t)], \quad k = 1, 2, \dots,$$
(3.1)

where $L_0^{(\beta)}(t) = 1$, $L_1^{(\beta)}(t) = 1 + \beta - t$. The basis set of the generalized OSLPs can be derived by using the following analytical expression

$$L_k^{(\beta)}(t) = \sum_{s=0}^k \frac{(-1)^s \Gamma(k+\beta+1) t^s}{\Gamma(k+\beta+1)(k-s)! s!}, \quad k = 0, 1, 2, \dots, n.$$
 (3.2)

Equation (3.2) can further be expressed as

$$L_{k}^{(\beta)}(t) = \sum_{s=0}^{k} \Omega_{(s,k)} t^{s}, \tag{3.3}$$

where

$$\Omega_{(s,k)} = \frac{(-1)^s \Gamma(k+\beta+1)}{\Gamma(k+\beta+1)(k-s)! s!}.$$
(3.4)

The basis set of generalized OSLPs $\{L_0^{\beta}(t), L_1^{\beta}(t), \dots, L_n^{\beta}(t)\}$ having the weight function $w(t) = e^{-t}t^{\beta}$, possesses the following property in the interval $[0, \infty)$:

$$\int_0^\infty L_i^{(\beta)}(t)L_j^{(\beta)}(t)w^{(\beta)}(t)dt = \delta_{ij}, \ i,j = 0,1,\dots,n,$$

where δ_{ij} is the kronecker delta function.

3.1. Function approximation via generalized OSLPs

A function f(t) that belongs to the class of square-integrable functions over the interval $[0, \infty)$ can be represented as the sum of generalized OSLPs as

$$u(t) = \sum_{j=0}^{\infty} c_j L_j^{(\beta)}(t), \tag{3.5}$$

where

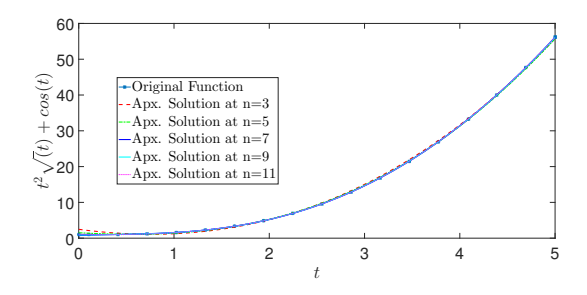
$$c_{j} = \frac{1}{h_{j}} \int_{0}^{\infty} u(t) w^{(\beta)}(t) L_{j}^{(\beta)}(t) dt, \quad j = 0, 1, 2, \dots$$
(3.6)

If we take the first n-terms of (3.5), then we have

$$u(t) \approx \sum_{j=0}^{n} c_j L_j^{(\beta)}(t) = F^T \psi(t), \tag{3.7}$$

where

$$F^{\mathsf{T}} = [c_0, c_1, c_2, \dots, c_n], \quad \psi(t) = [L_0^{(\beta)}(t), L_1^{(\beta)}(t), \dots, L_n^{(\beta)}(t)]^{\mathsf{T}}.$$



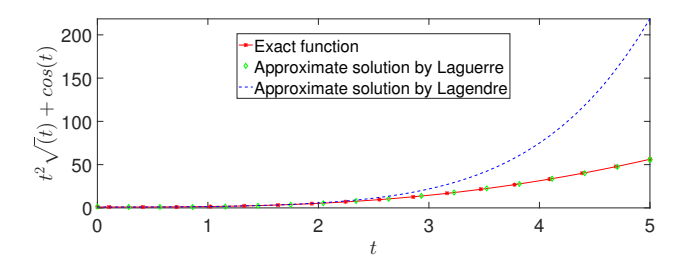


Figure 1: Graphical representation of function approximate by Laguerre polynomial for different values of n.

Figure 2: Graphical comparison of function approximate by Legendre and Laguerre polynomials for n = 5.

Figure 2 illustrates a graphical comparison of function approximation using Laguerre and Legendre polynomials for n=5, emphasizing the comparative efficacy of both orthogonal bases. The approximation utilizing Laguerre polynomials corresponds closely with the exact function $f(t)=t^2\sqrt(t)+\cos(t)$, especially as t varies. The higher efficiency results from the inherent applicability of Laguerre polynomials for problems defined on semi-infinite intervals, due to their orthogonality with respect to the weight function $e^{-t}t^{\beta}$. This property allows for a more realistic representation of functions exhibiting rapid growth or decay compared to Legendre polynomials, which are conventionally constructed on limited intervals such as [-1,1]. Thus, Laguerre-based spectral approximations reduce boundary-related errors and improve computational efficiency for functions exhibiting exponential characteristics or unbounded behavior, as demonstrated by the accuracy comparison illustrated in Figure 2.

4. Operational matrices of OSLPs

Lemma 4.1. The generalized Caputo derivative of $L_k^{(\beta)}(t)$, as defined in (3.3), can be computed as

$$_cD_{\alpha^+}^{\delta,\eta}L_k^{(\beta)}(t)=\sum_{s=\lceil\delta\rceil}^k\frac{(-1)^s(i!)\Gamma(k+\beta+1)\eta^\delta\Gamma(s/\eta+1)}{s!(s-k)!\Gamma(s+\beta+1)\Gamma(s/\eta-\delta+1)}t^{s-\eta\delta},\ \eta,\beta\in\mathbb{R}_+.$$

Proof. The result can be proven by using Eq. (3.3) and Definition 2.3.

Corollary 4.2. *For* $\delta > 0$, $s \in \mathbb{N}$, we have

$$_{RL}J_{0^{+}}^{\delta,\eta}t^{s}=\eta^{-\delta}\frac{\Gamma(s/\eta+1)}{\Gamma(s/\eta+\delta+1)}t^{s+\eta\delta}\text{, }\delta,\eta\in\mathbb{R}_{+}.$$

Lemma 4.3. For any $t^{s+\eta\delta} \in L^2([0,\infty);e^{-t}t^{\beta})$, we have the following result:

$$\begin{split} t^{s+\eta\delta} &\approx \sum_{j=0}^n b_j L_j^{(\beta)}(t), \ \delta, \eta, \beta \in \mathbb{R}_+, \\ b_j &= \sum_{l=0}^j \frac{(-1)^l j!}{l!(j-l)! \Gamma(l+\beta+1)} \Gamma(s+\eta\delta+\beta+l+1). \end{split} \tag{4.1}$$

Proof. Taking (n+1)-terms of OSLPs, we can approximate $t^{s-\eta\delta}$ as

$$t^{s+\eta\delta} \approx \sum_{j=0}^{n} b_{j} L_{j}^{\beta}(t).$$

Using Eq. (3.6), we may determine b_i as

$$\begin{split} b_{j} &= \sum_{l=0}^{j} \frac{(-1)^{l} j!}{l! (j-l)! \Gamma(l+\beta+1)} \int_{0}^{\infty} e^{-t} t^{s+\eta\delta+\beta+l} dt, \\ b_{j} &= \sum_{l=0}^{j} \frac{(-1)^{l} j!}{l! (j-l)! \Gamma(l+\beta+1)} \Gamma(s+\eta\delta+\beta+l+1). \end{split} \tag{4.2}$$

Eqs. (4.1) and (4.2) establish the result.

4.1. Generalized FOIOM of OSLPs in RL-sense

The operational matrices corresponding to orthogonal polynomials have a crucial significance in several areas of applied mathematics, especially in the field of computational mathematics. By applying operational matrices based on orthogonal polynomials, it becomes feasible to express differential and integral operators as matrix operations. Consequently, FODEs could be converted into SAEs, considerably simplifying the task of obtaining numerical solutions. This section focuses on the construction of a new generalized FOIOM based on the generalized RL operator.

Theorem 4.4. Let $\psi(t) = [L_0^{\beta}(t), L_1^{\beta}(t), \dots, L_n^{\beta}(t)]^T$, then the following holds true

$$J^{\delta,\eta}L_k^{\beta}(t) \approx Q^{(\delta,\eta)}\psi(t),$$

where $Q^{(\delta,\eta)}$ is $(n+1)\times (n+1)$ and is the generalized FOIOM of order $\delta\in\mathbb{R}_+$,

$$\begin{split} Q_{(n+1,n+1)}^{\delta,\eta} &= \sum_{k=0}^s \Upsilon_{(s,l,k)}, \ s=0,\dots,n, \ l=0,1,\dots,n, \\ \Upsilon_{(s,l,k)} &= \sum_{l=0}^j \frac{(-1)^{s+l}(j!)\eta^{\delta}\Gamma(k+\beta+1)\Gamma(s/\eta+1)\Gamma(s+\eta\delta+\beta+l+1)}{(l!)(s!)(k-s)!(j-l)!\Gamma(s+\beta+1)\Gamma(s/\eta+\delta+1)\Gamma(l+\beta+1)}. \end{split}$$

Proof. Using the GFI operator introduced in Eqs. (2.2)-(3.4), we have

$$_{RL}J^{\delta,\eta}L_{k}^{\beta}(t) = \sum_{s=0}^{k} \Omega_{(s,k)} _{RL}J^{\delta,\eta} t^{s}. \tag{4.3}$$

Using Corollary 4.2, Eq. (4.3) can be expressed as

$$_{RL}J^{\delta,\eta}L_{k}^{\beta}(t) = \sum_{s=0}^{k} \Omega_{(s,k)}\eta^{-\delta} \frac{\Gamma(s/\eta + 1)}{\Gamma(s/\eta + \delta + 1)} t^{s+\eta s}. \tag{4.4}$$

Using (n + 1)-terms of OSLPs, $t^{s+\eta s}$ can be approximated as

$$t^{s+\eta s} \approx \sum_{j=0}^{n} b_j L_j^{\beta}(t). \tag{4.5}$$

Using Lemma 4.3, Eq. (4.5) can be expressed as

$$t^{s+\eta s} = \sum_{i=0}^{n} \left(\sum_{l=0}^{j} \frac{(-1)^{l} j!}{(l!)(j-l)! \Gamma(l+\beta+1)} \Gamma(s+\eta \delta+l+1) \right) L_{j}^{(\beta)}(t). \tag{4.6}$$

Using Eq. (3.4) and Eq. (4.6) in Eq. (4.4), we have

$$\begin{split} {}_{RL}J^{\delta,\eta}L_{k}^{\beta}(t) &\simeq \sum_{s=0}^{k} \frac{(-1)^{s}\Gamma(k+\beta+1)}{s!(k-s)!} \eta^{\delta} \frac{\Gamma(s/\eta+1)}{\Gamma(s/\eta+\delta+1)} \\ &\times \sum_{j=0}^{n} \left(\sum_{l=0}^{j} \frac{(-1)^{l}j!}{l!(j-l)!\Gamma(l+\beta+1)} \Gamma(s+\eta\delta+l+1) \right) L_{j}^{(\beta)}(t). \end{split} \tag{4.7}$$

Eq. (4.7) can further be written as

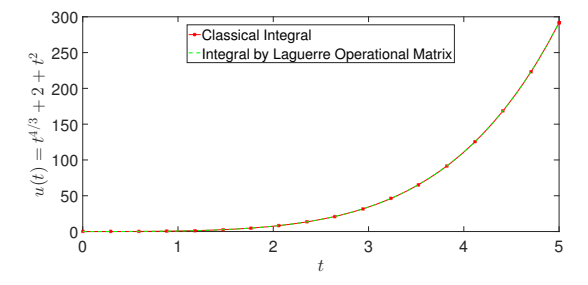
$$_{RL}J^{\delta,\eta}L_k^\beta(t)\simeq \left[\sum_{s=0}^k \Upsilon_{(s,0,k)} \ \sum_{s=0}^k \Upsilon_{(s,1,k)} \ \sum_{k=\lceil\alpha\rceil}^k \Upsilon_{(s,2,k)},\ldots, \sum_{s=0}^k \Upsilon_{(s,n,k)}\right]\psi(t),$$

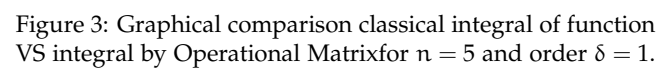
where

$$\Upsilon_{(s,l,k)} = \sum_{l=0}^j \frac{(-1)^{s+l}(j!)\eta^{\delta}\Gamma(k+\beta+1)\Gamma(s/\eta+1)\Gamma(s+\eta\delta+\beta+l+1)}{(l!)(s!)(k-s)!(j-l)!\Gamma(s+\beta+1)\Gamma(s/\eta+\delta+1)\Gamma(l+\beta+1)}.$$

Hence the result is proved,

$$Q_{(6,6)}^{1,1} = \begin{bmatrix} 2 & -1 & 0 & 0 & 0 & 0 \\ 1 & 1 & -1 & 0 & 0 & 0 \\ 1 & 0 & 1 & -1 & 0 & 0 \\ 1 & 0 & 0 & 1 & -1 & 0 \\ 1 & 0 & 0 & 0 & 1 & -1 \\ 1 & 0 & 0 & 0 & 0 & 1 \end{bmatrix}, \quad Q_{(7,7)}^{4/3,1} = \begin{bmatrix} \frac{9}{4} & -\frac{43}{32} & \frac{15}{128} & \frac{49}{2048} & \frac{65}{8192} & \frac{231}{65536} & \frac{493}{262144} \\ \frac{5}{4} & \frac{27}{32} & -\frac{165}{128} & \frac{285}{2048} & \frac{243}{8192} & \frac{735}{65536} & \frac{1419}{262144} \\ \frac{5}{4} & -\frac{5}{32} & \frac{128}{128} & -\frac{2595}{2048} & \frac{1203}{8192} & \frac{2175}{65536} & \frac{3435}{262144} \\ \frac{5}{4} & -\frac{5}{32} & -\frac{128}{128} & \frac{2013}{2048} & \frac{10317}{8192} & \frac{9855}{65536} & \frac{262144}{262144} \\ \frac{5}{4} & -\frac{5}{32} & -\frac{5}{128} & -\frac{35}{2048} & \frac{8115}{8192} & -\frac{82305}{65536} & \frac{39915}{262144} \\ \frac{5}{4} & -\frac{32}{32} & -\frac{128}{128} & -\frac{3048}{2048} & \frac{8192}{8192} & \frac{65536}{65536} & \frac{262144}{262144} \\ \frac{5}{4} & -\frac{32}{32} & -\frac{128}{128} & -\frac{3048}{2048} & \frac{8192}{8192} & \frac{65536}{65536} & \frac{262144}{262144} \\ \frac{5}{4} & -\frac{32}{32} & -\frac{128}{128} & -\frac{3048}{2048} & \frac{8192}{8192} & \frac{65536}{65536} & \frac{262144}{262144} \\ \frac{5}{4} & -\frac{32}{32} & -\frac{128}{128} & -\frac{3048}{2048} & \frac{8192}{8192} & \frac{65536}{65536} & \frac{262144}{262144} \\ \frac{5}{4} & -\frac{32}{32} & -\frac{128}{128} & -\frac{3048}{2048} & \frac{8192}{8192} & \frac{65536}{65536} & \frac{262144}{262144} \\ \frac{5}{4} & -\frac{32}{32} & -\frac{128}{128} & -\frac{31}{2048} & \frac{8192}{8192} & \frac{65536}{65536} & \frac{262144}{262144} \\ \frac{5}{4} & -\frac{32}{32} & -\frac{128}{128} & -\frac{31}{2048} & \frac{8192}{8192} & \frac{65536}{65536} & \frac{262144}{262144} \\ \frac{5}{4} & -\frac{32}{32} & -\frac{128}{128} & -\frac{31}{2048} & \frac{8192}{8192} & \frac{65536}{65536} & \frac{262144}{262144} \\ \frac{5}{4} & -\frac{32}{32} & -\frac{128}{128} & -\frac{31}{2048} & \frac{8192}{8192} & \frac{65536}{65536} & \frac{262144}{262144} \\ \frac{5}{4} & -\frac{32}{32} & -\frac{128}{128} & -\frac{31}{2048} & \frac{8192}{8192} & \frac{65536}{65536} & \frac{262144}{262144} \\ \frac{5}{4} & -\frac{32}{32} & -\frac{128}{128} & -\frac{31}{2048} & \frac{8192}{8192} & \frac{65536}{65536} & \frac{262144}{262144} \\ \frac{5}{4} & -\frac{32}{32} & -\frac{128}{128} & -\frac{31}{2048} & \frac{8192}{8192} & \frac{65536}{65536} & \frac{262144}{262144} \\ \frac{5}{4} & -\frac{32}{32} & -\frac{128}{128} & -\frac{31$$





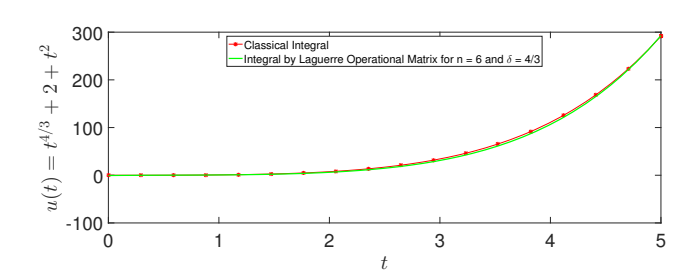


Figure 4: Graphical comparison classical integral of function VS integral by Operational Matrix for n=6 and order $\delta=4/3$.

Figures 3 and 4 present graphical comparisons between the classical integral of the functions and their numerical approximations obtained using the Laguerre integral operational matrix. The graphs clearly show that the results produced by the operational matrix method closely align with the classical integrals, highlighting its high accuracy and reliability.

4.2. Sylvester matrix equation

The Sylvester matrix equation is a matrix equation of the form: AX + XB = C, where $A \in \mathbb{R}^{m \times m}$, $B \in \mathbb{R}^{n \times n}$, and $C \in \mathbb{R}^{m \times n}$ are known matrices. The objective is to determine the unknown matrix $X \in \mathbb{R}^{m \times n}$ that satisfies this relation. According to Sylvester's theorem [17], a unique solution exists if and only if the sets of eigenvalues of matrices A and B are disjoint. That is $\alpha(A) \cap \alpha(B) = \emptyset$, where $\alpha(A)$ and $\alpha(B)$ denote the spectra of A and B, respectively. This equation has widespread applications in several fields such as control theory for analyzing system behavior, model order reduction for simplifying large dynamic systems, and signal processing for improving signal quality. It is also valuable in image restoration, system decoupling, and implicit numerical schemes used in solving differential equations. For a detailed discussion, refer to [9, 11, 12].

5. Numerical approach

Consider the following FODEs subject to the initial conditions (ICs)

$${}_{C}D^{\delta,\eta}\mathfrak{u}(t)=\mathsf{f}\left(\mathsf{t},\mathfrak{u}(t),{}_{C}D^{\delta_{1},\eta_{1}}\mathfrak{u}(t),{}_{C}D^{\delta_{2},\eta_{2}}\mathfrak{u}(t),\ldots,{}_{C}D^{\delta_{n},\eta_{n}}\mathfrak{u}(t)\right),\ \mathfrak{u}^{(\mathfrak{i})}(0)=\lambda_{\mathfrak{i}},\ \mathfrak{i}=0,1,\ldots,\lceil\delta\rceil-1.\ \ (5.1)$$

Consider the following approximation holds true

$${}_{C}D_{\alpha}^{\delta,\eta}\mathfrak{u}(\mathfrak{t}) = \mathsf{F}^{\mathsf{T}}\psi(\mathfrak{t}). \tag{5.2}$$

Using the GFI operator of order δ together with the ICs to Eq. (5.2), we get

$$u(t) = F^{\mathsf{T}} Q^{\delta,\eta} \psi(t) + \sum_{i=0}^{\lceil \delta \rceil - 1} \frac{\lambda_i}{i!} t^i.$$
 (5.3)

Now

$$\begin{split} D^{\delta_1,\eta_1}u(t) &= D^{\delta_1,\eta_1}[F^TQ^{\delta,\eta}\psi(t) + \sum_{i=0}^{\lceil \delta \rceil-1} \frac{\lambda_i}{i!}D^{\delta_1,\eta_1}t^i] \\ &= F^TQ^{(\delta-\delta_1),\eta_1}\psi(t) + \sum_{i=\lceil \delta_1 \rceil}^{\lceil \delta \rceil-1} \frac{\lambda_i}{\Gamma(i-\delta_1+1)}t^{i-\delta_1}, \ \delta_1 < \lceil \delta \rceil - 1, \\ D^{\delta_2,\eta_2}u(t) &= D^{\delta_2,\eta_2}[F^TQ^{\delta,\eta}\psi(t) + \sum_{i=0}^{\lceil \delta \rceil-1} \frac{\lambda_i}{i!}D^{\delta_2,\eta_2}t^i] \\ &= F^TQ^{(\delta-\delta_2)\eta_2}\psi(t) + \sum_{i=\lceil \delta_2 \rceil}^{\lceil \delta \rceil-1} \frac{\lambda_i}{\Gamma(i-\delta_2+1)}t^{i-\delta_2}, \ \delta_2 < \lceil \delta \rceil - 1. \end{split}$$

Generally we can write it as

$$\begin{split} D^{\delta_{\mathfrak{m}},\eta_{\mathfrak{m}}}\mathfrak{u}(t) &= D^{\delta_{\mathfrak{m}},\eta_{\mathfrak{m}}}[\mathsf{F}^\mathsf{T}Q^{\delta,\eta}\psi(t) + \sum_{i=0}^{\lceil \delta \rceil-1}\frac{\lambda_{i}}{i!}D^{\delta_{\mathfrak{m}},\eta_{\mathfrak{m}}}t^{i}] \\ &= \mathsf{F}^\mathsf{T}Q^{(\delta-\delta_{\mathfrak{m}}),\eta_{\mathfrak{m}}}\psi(t) + \sum_{i=\lceil \delta_{\mathfrak{m}} \rceil}^{\lceil \delta \rceil-1}\frac{\lambda_{i}}{\Gamma(i-\delta_{\mathfrak{m}}+1)}t^{i-\delta_{\mathfrak{m}}}, \ \delta_{\mathfrak{m}} < \lceil \delta \rceil - 1, \end{split} \tag{5.4}$$

where

$$\sum_{i=\lceil \delta_m \rceil}^{\lceil \delta \rceil-1} \frac{\lambda_i}{\Gamma(i-\delta_m+1)} t^{i-\delta_m} = G_m^T \psi(t).$$

Now approximating the second term of Eq. (5.4), we get

$$G_{\mathfrak{m}}^{\mathsf{T}}\psi(\mathfrak{t}) = \sum_{\mathfrak{i}=\lceil\delta_{\mathfrak{j}}\rceil}^{\lceil\delta\rceil-1} \frac{\lambda_{\mathfrak{i}}}{\Gamma(\mathfrak{i}-\delta_{\mathfrak{j}}+1)} \Bigg(\sum_{q=0}^{\mathfrak{m}} \Big(\sum_{s=0}^{q} \frac{(-1)^{q} q!}{\Gamma(s+\delta+1)(q-s)! s!} \Gamma(\mathfrak{i}-\delta_{\mathfrak{j}}+\beta+s+1)\Big)\Bigg),$$

 $\delta_j < \lceil \delta \rceil - 1, j = 1, 2, \ldots, m.$ Eq. (5.4) becomes

$$D^{\delta_{\mathfrak{m}},\eta_{\mathfrak{m}}}u(t) = F^{\mathsf{T}}Q^{(\delta-\delta_{\mathfrak{m}}),\eta_{\mathfrak{m}}}\psi(t) + G_{\mathfrak{m}}^{\mathsf{T}}\psi(t). \tag{5.5}$$

the term in (5.3) can be evaluated as

$$\sum_{i=0}^{\lceil \delta \rceil -1} \frac{\lambda_i}{i!} t^i \approx \sum_{p=0}^n e_j L_j^\beta(t) = R_p^T \Psi(t).$$

so,

$$u(t) = F^{T}Q^{\delta,\eta}\psi(t) + R_{p}^{T}\Psi(t), \quad p = 0, 1, ..., n.$$
 (5.6)

Similarly the sourse term g(t) can be evaluated by the basis of generalized OSLPs as

$$g(t) \approx \sum_{j=0}^{n} b_{j} L_{j}^{\beta}(t) = B_{j}^{\mathsf{T}} \psi(t),$$
 (5.7)

The B_i^T can be evaluated by using (3.6). Using Eqs. (5.2), (5.5), (5.6), and (5.7), Eq. (5.1) becomes

$$F_{(1\times n+1)}^{\mathsf{T}} + F_{(1\times n+1)}^{\mathsf{T}} \left(Q_{(n+1\times n+1)}^{(\delta-\delta_{\mathfrak{m}},\eta_{\mathfrak{m}})} + Q_{(n+1\times n+1)}^{(\delta,\eta_{\mathfrak{m}})} \right) = -G_{(1\times n+1)}^{\mathsf{T}} - R_{(1\times n+1)}^{\mathsf{T}} + B_{(1\times n+1)}^{\mathsf{T}}.$$
 (5.8)

Eq. (5.8) can further be simplified into Sylvester-type matrix equations AX + XB = C, which can be easily solved for unknowns $F_{(1\times n+1)}^T$ by substituting the values of $F_{(1\times n+1)}^T$ and $G_{(1\times n+1)}^T$ in Eq. (5.3), we get the approximation of the problem given in Eq. (5.1).

6. Examples

Example 6.1. Consider the following FODEs of Bagley-Torvik type associated with the ICs [22–24, 27],

$${}_{C}\mathcal{D}^{\delta,\eta}\mathfrak{u}(t)+{}_{C}\mathcal{D}^{\delta_{1},\eta_{1}}\mathfrak{u}(t)+\mathfrak{u}(t)=H(t),\quad 1<\delta_{1}<2,\ t\in[0,1],\ \mathfrak{u}(0)=\lambda_{0},\ \mathfrak{u}'(0)=\lambda_{1},$$

for $\delta=2$, $\delta_1=3/2$, $\eta=\eta_1=1$, $\lambda_0=\lambda_1=1$, and H(t)=1+t. The exact solution expresses as $\mathfrak{u}(t)=1+t$. By implementing the PNM discussed in Section 4, we have

$$_{C}\mathcal{D}^{2}u(t) = F^{T}\psi(t). \tag{6.1}$$

Using Eq. (5.3), we can express Eq. (6.1) in the following way

$$u(t) \approx F^{T} Q_{(3,3)}^{(2)} \psi(t) + 1 + t.$$
 (6.2)

The expression 1 + t in Eq. (6.2) can be approximated by Eq. (3.7). Table 1 illustrates the absolute error of Example 6.1 for different values of n after implementing our PNM. It shows that the exact and the approximate solution matches upto 14 decimal places. The results highlight the efficiency and accuracy of our PNM.

	Table 1. The absolute error of Example 0.1, using 11vivi for various values of it.							
t	n = 5	n = 10	n = 15	n = 20	n = 25			
0	4.1925×10^{-12}	8.9100×10^{-13}	2.7409×10^{-14}	6.7951×10^{-14}	3.7912×10^{-14}			
0.2	1.5681×10^{-12}	6.994×10^{-14}	7.8197×10^{-15}	1.4162×10^{-15}	1.2183×10^{-14}			
0.4	1.0990×10^{-14}	2.1940×10^{-13}	1.0357×10^{-13}	6.8015×10^{-14}	8.5713×10^{-14}			
0.6	6.1928×10^{-13}	4.1749×10^{-13}	3.7444×10^{-13}	3.3172×10^{-13}	$3.34.3 \times 10^{-13}$			
0.8	3.2747×10^{-13}	8.4649×10^{-13}	9.2585×10^{-13}	8.9611×10^{-13}	8.8994×10^{-13}			
1.0	7.9773×10^{-13}	1.7314×10^{-12}	1.8917×10^{-12}	1.8785×10^{-12}	1.8737×10^{-12}			

Table 1: The absolute error of Example 6.1, using PNM for various values of n.

Table 2: Comparing the results of Example 6.1 based on algorithm execution time(s)

n	Execution time (s)				
	PNM Algorithm [7]				
5	24.08				
10	26.17	261.19			
15	55.32	1427.78			
20	99.62	5467.58			

Table 2 presents a comparison of the execution timings for Example 6.1 that uses our PNM and the technique described in [7]. The investigation examines several values of n. The technique described in reference [7] applied a hybrid methodology by combining the operational matrix of fractional-order integrals for generalized OSLPs in RL definition and the Tau method. Table 2 clearly shows that the execution time data for both techniques exhibit unique characteristics related to performance. When the value of n is 5, the PNM has an execution time of 10.51 seconds, but the approach described in [7] requires 24.08 seconds. As the value of n grows to 20, the execution time of the PNM method is 99.62 seconds, whereas the technique mentioned in [7] encounters a more significant rise.

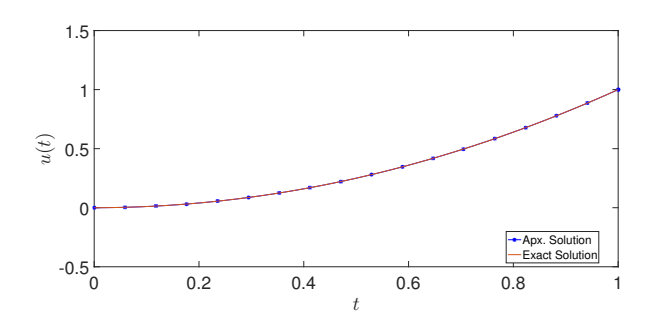
Example 6.2. Consider the following FODEs with the ICs [6],

$${}_{C}\mathcal{D}^{\delta,\eta}\mathfrak{u}(t) + {}_{C}\mathcal{D}^{\delta_{1},\eta_{1}}\mathfrak{u}(t) + \mathfrak{u}(t) = H(t), \ 0 < \delta_{1} \leqslant 1, \ t \in [0,\infty), \ \mathfrak{u}(0) = \lambda_{0}, \ \mathfrak{u}'(0) = \lambda_{1},$$

where $\delta=2$, $\delta_1=1/2$, $\eta=\eta_1=1$, and $H(t)=t^2+2+\frac{2.6666666667}{\Gamma(0.5)}t^{1.5}$. The exact solution is expressed as $u(t)=t^2$. Table 3 shows that as the number of terms n in the generalized SLP increases, the absolute error decreases significantly, which indicates accuracy and the stability of PNM. In Figure 6 the resemblance between the approximate and solution is analyzed for fixed $\eta=1$ and $0<\delta_1<1$. Figure 7 illustrates the error behavior of the proposed method for Example 6.2 by graphing the absolute error against the time variable t, for different values of n. The error remains low (on the order of 10^{-12}) throughout the interval [0,1], and decreases more as n grows, confirming the method's excellent accuracy and spectrum convergence. The graphic demonstrates the suggested approach's reliability in capturing solution behavior with little numerical error.

Table 3: The absolute error of Example 6.2, using PNM at different values of n.

			1 0		
t	n = 5	n = 10	n = 15	n = 20	n = 25
0	4.1925×10^{-12}	8.9100×10^{-13}	2.7409×10^{-14}	6.7951×10^{-14}	3.7912×10^{-14}
0.2	1.5681×10^{-12}	6.994×10^{-14}	7.8197×10^{-15}	1.4162×10^{-15}	1.2183×10^{-14}
0.4	1.0990×10^{-14}	2.1940×10^{-13}	1.0357×10^{-13}	6.8015×10^{-14}	8.5713×10^{-14}
0.6	6.1928×10^{-13}	4.1749×10^{-13}	3.7444×10^{-13}	3.3172×10^{-13}	$3.34.3 \times 10^{-13}$
0.8	3.2747×10^{-13}	8.4649×10^{-13}	9.2585×10^{-13}	8.9611×10^{-13}	8.8994×10^{-13}
1.0	7.9773×10^{-13}	1.7314×10^{-12}	1.8917×10^{-12}	1.8785×10^{-12}	1.8737×10^{-12}



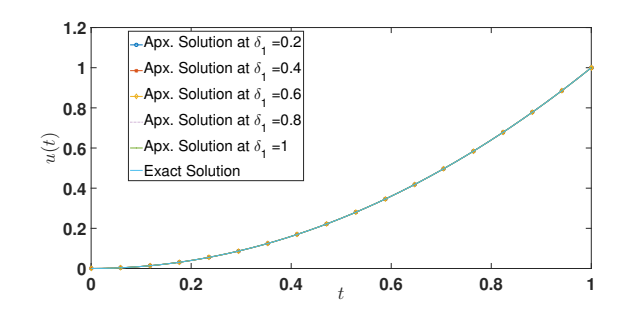


Figure 5: Graph of the exact and approximate solution of Example 6.2.

Figure 6: Graphical representation of the solution curve of Example 6.2 for the various values of δ_1 .

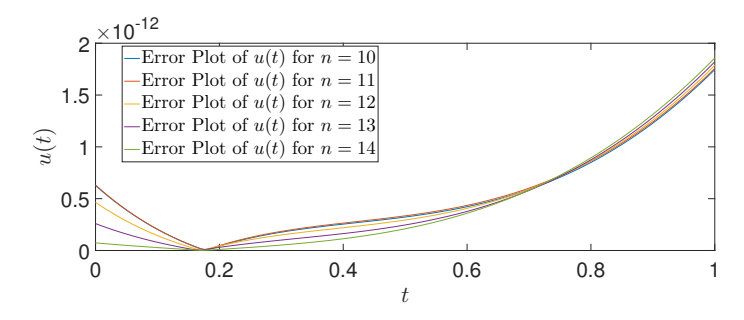


Figure 7: Graphical representation of the error of Example 6.2 for various value of n.

Example 6.3. Consider the following FODEs with the ICs [6]:

$${}_{C}\mathfrak{D}^{\delta,\eta}\mathfrak{u}(t) + 3\mathfrak{u}(t) = H(t), \ 0 < \delta_{1} \leqslant 1, \ 0 < \eta \leqslant 1, \ t \in [0,\infty), \ \mathfrak{u}(0) = \lambda_{0}, \ \mathfrak{u}'(0) = \lambda_{1},$$

where $\delta=3/2$, $\eta=1$, and $H(t)=3t^3+\frac{8}{\Gamma(0.5)}t^{1.5}$. The exact solution is given as $u(t)=t^3$. Example 6.3 exhibits the accuracy of PNM in solving FODEs. Figure 8 compares the exact and approximate solution curves. Figure 9 shows the solution curves for several values of the parameter η , the approximate solutions remain closely aligned with the exact solution which demonstrate the method's adaptability and accuracy under changing parameters. Figure 10 shows the solution curves for various values of δ_1 . Once again, the approximation agrees with the exact solution, proving the PNM's stability across different order and parameter choices. These figures demonstrate the method's accuracy and applicability in solving complex FODEs. Table 4 compares the algorithm execution time (in seconds) between the proposed technique and the algorithm described in [14], as measured for various values of η . The proposed method uses substantially less CPU time than the algorithm in [14], highlighting the efficiency of the proposed methodology.

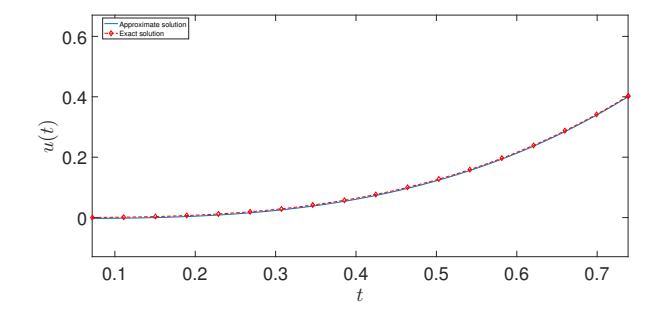


Figure 8: Graph of the exact and approximate solution of Example 6.3.

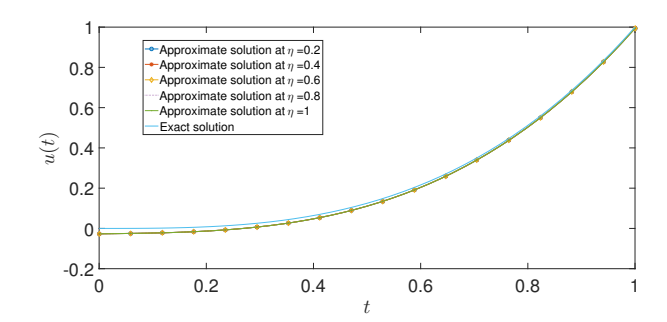


Figure 9: Graph of the exact and approximate solution for the various values of η of Example 6.3.

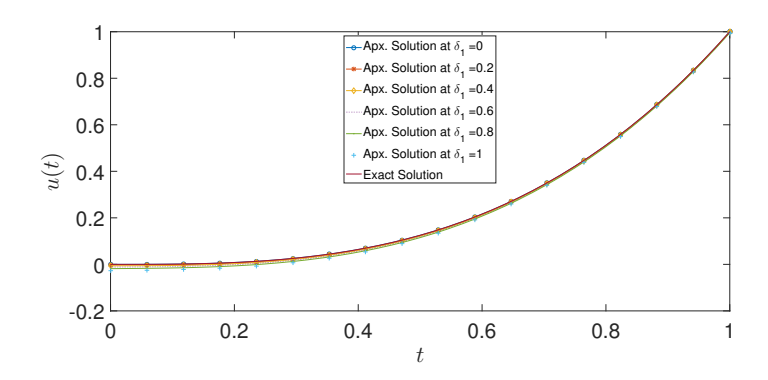


Figure 10: Graph of the exact and approximate solution for the various values of δ_1 of Example 6.3.

Table 4: Comparing the results of Example 6.3 based on Algorithm Execution Time(s), as measured by both the PNM and the algorithm proposed in [7].

n	Appro	ximate solution	Execution time (s)		
	PNM Algorithm [7]		PNM	Algorithm [7]	
3	t ³	t ³	4.95	7.34	
5	t^3	t^3	6.41	21.16	
10	t^3	t^3	14.39	244.98	
13	t^3	t^3	23.16	759.52	
15	t^3	t^3	28.20	1384.75	

Example 6.4. Consider the following FODEs of Bagley-Torvik type associated with the ICs [6]:

$${}_{C}\mathcal{D}^{\delta,\eta}u(t) + 2{}_{C}\mathcal{D}^{\delta_1,\eta_1}u(t) + {}_{C}\mathcal{D}^{\delta_2,-\eta_2}u(t) + u(t) = H(t), \quad t \in [0,\infty), \quad u(0) = \lambda_0, \quad u'(0) = \lambda_1, \quad u'($$

where $\delta=2$, $\delta_1=1$, $\delta_2=1/2$, $\eta=\eta_1=\eta_2=1$, $\lambda_0=\lambda_1=0$, and $H(t)=t^7+\frac{2048}{429\sqrt{\pi}}t^{6.5}-14t^6-t^2-\frac{8}{3\sqrt{\pi}}t^{1.5}+4t-2$. The exact solution is $u(t)=t^7-t^2$. Example 6.4 demonstrates the proposed accuracy and efficiency in solving FODEs. Figure 11 presents a comparison that how approximate solution closely matches to the exact one, showcasing the method's precision. Table 5 shows absolute error levels over time for different numbers of terms n in the generalized Laguerre polynomial. As the number of terms grows, the absolute error between exact and approximation answers decreases considerably. This decreasing errors demonstrate the method's reliability in solving complex FODEs with a high level of accuracy. In the Table 6, the accuracy of the proposed method is evaluated using standard error metrics: maximum norm error ($\|NE\|_{\infty}$), mean error (ME), root mean square error (RMSE), and significant correct digits (SCD), calculated for different values of n. For each case, the RMSE serves as the reference measure of error, and assuming nearly uniform point-wise errors, both ME and $\|NE\|_{\infty}$ are considered approximately equal to the RMSE. The corresponding SCD values are then computed accordingly. The results demonstrate that the method maintains a high level of accuracy and numerical precision across different values of n.

Table 5: The absolute error is calculated using our PNM for different values of n of Example 6.4.

t	n = 7	n = 10	n = 13
0	1.4142×10^{-8}	3.2401×10^{-7}	4.2574×10^{-8}
0.2	5.8276×10^{-9}	9.0934×10^{-8}	6.0305×10^{-9}
0.4	4.4458×10^{-10}	2.1998×10^{-8}	6.1579×10^{-9}
0.6	2.6813×10^{-9}	5.7735×10^{-8}	6.1519×10^{-9}
0.8	4.1262×10^{-9}	4.8470×10^{-8}	1.5500×10^{-9}
1.0	4.3774×10^{-9}	1.7549×10^{-8}	3.3151×10^{-9}

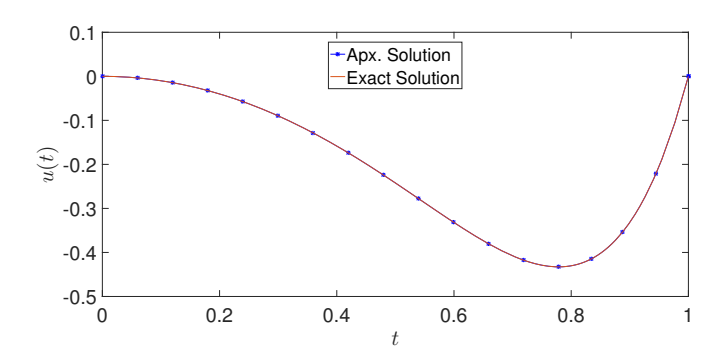


Figure 11: Graphical visualization of the exact and approximate solutions for the given example. 6.4.

Table 6: The distribution of errors and precision factor (SCD) in Example 6.4 for different n values.

				,	· / 1			
n	. NE ∞	Time (sec)	RMSE	Time (sec)	ME	Time (sec)	SCD	Time (sec)
10	3.2401×10^{-7}	(25.2258)	1.2163×10^{-7}	(25.2796)	8.2847×10^{-8}	(25.3021)	6.4894	(25.1524)
12	$2 3.0264 \times 10^{-8}$	(33.4243)	1.0784×10^{-8}	(33.8622)	6.7468×10^{-9}	(42.6438)	7.5191	(33.6689)
14	$1 2.8724 \times 10^{-8}$	(56.4592)	9.862×10^{-9}	(55.4129)	5.9837×10^{-9}	(43.8059)	7.5418	(43.9162)

7. Conclusion

We present a numerical algorithm based on the newly developed FOIOM of OSLPs within the RL framework. The proposed method demonstrates significantly improved accuracy compared to the STM. To assess its performance, we solve various FODEs and compare the results of our PNM with those obtained using the STM [7]. The comparison highlights that our method achieves accurate results when compared with the STM. Furthermore, the proposed approach efficiently converts FODEs into Sylvester-type equations can be solved efficiently using MatLab. This study can be further extended to address nonlinear FODEs, partial differential equations (PDEs), and boundary value problems (BVPs). For nonlinear FODEs and PDEs, the construction of a new integral operational matrix will be necessary, while solving BVPs will require the development of new product operational matrix. In addition, extending the method to BVPs would involve modifications to the formulation to appropriately incorporate boundary conditions. These extensions could present further challenges, such as increased computational cost and complexities, which can be explored in future research.

7.1. Limitations of the proposed numerical method

The proposed method, utilizing the FOIOM of OSLPs within the Riemann-Liouville framework, demonstrates consistent efficacy for linear fractional initial value problems (FIVPs). However, it presents substantial limitations in terms of applicability, scope, and computational factors.

Limited applicability to nonlinear problems. The current formulation of the method is developed specifically for linear FODEs. The absence of a generalized framework to construct operational matrices that effectively manage nonlinear terms restricts its direct application to nonlinear problems. This limitation hinders the use of the method in more complex real-world systems when non-linearity occurs frequently.

Confined to FIVPs. The method is specifically formulated for FIVPs and is not applicable to BVPs. Extending it to handle BVPs would require the construction of a product operational matrix, a concept not explored in this study. As a result, the practical applicability of the method remains confined.

Recommendation. We recommend the proposed method as an effective and accurate approach for solving linear FIVPs, particularly when high precision is required. To expand its utility, future research should focus on adapting the method to nonlinear and BVPs by developing suitable product operational matrices and incorporating adaptive solution strategies. Such advancements could significantly broaden the method's applicability and impact in the field of FODEs.

Data avaiabilty

All data generated or analyzed during this study are available from the corresponding author on reasonable request. No proprietary or restricted data were used.

Funding

The authors declare that this work received no funding support.

Acknowledgement

This article has been supported by EU funds under the project "Increasing the resilience of power grids in the context of decarbonisation, decentralisation and sustainable socioeconomic development", CZ.02.01.01/00/23_021/0008759, through the Operational Programme Johannes Amos Comenius.

References

- [1] M. Abramowitz, I. A. Stegun, *Handbook of mathematical functions with formulas, graphs, and mathematical tables*, U. S. Government Printing Office, Washington, DC, (1964).
- [2] A. Atangana, D. Baleanu, New fractional derivatives with nonlocal and non-singular kernel: theory and application to heat transfer model, arXiv preprint arXiv:1602.03408 (2015), 8 pages. 2
- [3] R. H. Bartels, G. W. Stewart, *Algorithm 432 [C2]: Solution of the matrix equation* AX + XB = C [F4], Commun. ACM, **15** (1972), 820–826.
- [4] A. H. Bhrawy, M. A. Alghamdi, *The operational matrix of Caputo fractional derivatives of modified generalized Laguerre polynomials and its applications*, Adv. Differ. Equ., **2013** (2013), 19 pages. 1
- [5] A. H. Bhrawy, Y. A. Alhamed, D. Baleanu, A. A. Al-Zahrani, New spectral techniques for systems of fractional differential equations using fractional-order generalized Laguerre orthogonal functions, Fract. Calc. Appl. Anal., 17 (2014), 1137–1157.
- [6] A. H. Bhrawy, D. Baleanu, L. M. Assas, J. A. T. Machado, On a generalized Laguerre operational matrix of fractional integration, Math. Probl. Eng., 2013 (2013), 7 pages. 1, 6.2, 6.3, 6.4
- [7] A. H. Bhrawy, T. M. Taha, An operational matrix of fractional integration of the Laguerre polynomials and its application on a semi-infinite interval, Math. Sci. (Springer), 6 (2012), 7 pages. 1, 2, 6.1, 4, 7
- [8] S. Boulaaras, R. Jan, V.-T. Pham, *Recent advancement of fractional calculus and its applications in physical systems*, Eur. Phys. J. Spec. Top., **232** (2023), 2347–2350. 1
- [9] D. Calvetti, L. Reichel, *Application of ADI iterative methods to the restoration of noisy images*, SIAM J. Matrix Anal. Appl., 17 (1996), 165–186. 4.2
- [10] L. Debnath, Recent applications of fractional calculus to science and engineering, Int. J. Math. Math. Sci., 2003 (2003), 3413–3442. 1
- [11] M. A. Epton, Methods for the solution of AXD BXC = E and its application in the numerical solution of implicit ordinary differential equations, BIT, **20** (1980), 341–345. 4.2
- [12] G. H. Golub, C. F. Van Loan, Matrix computations, Johns Hopkins University Press, Baltimore, MD, (2013). 4.2
- [13] R. Hilfer, *Local porosity theory and stochastic reconstruction for porous media*, In: Statistical physics and spatial statistics (Wuppertal, Springer, Berlin, (2000). 2
- [14] R. Hilfer, Applications of fractional calculus in physics, World Scientific Publishing Co., River Edge, NJ, (2000). 6.3
- [15] U. N. Katugampola, New approach to a generalized fractional integral, Appl. Math. Comput., 218 (2011), 860–865. 2
- [16] A. A. Kilbas, H. M. Srivastava, J. J. Trujillo, *Theory and applications of fractional differential equations*, Elsevier Science B.V., Amsterdam, (2006). 2
- [17] P. Lancaster, M. Tismenetsky, The theory of matrices: with applications, Academic Press, New York, (1985). 4.2
- [18] K. S. Miller, B. Ross, An introduction to the fractional calculus and fractional differential equations, John Wiley & Sons, New York, (1993). 2
- [19] C. Min, Y. Chen, Semi-classical Jacobi polynomials, Hankel determinants and asymptotics, Anal. Math. Phys., 12 (2022), 25 pages.
- [20] I. Podlubny, An introduction to fractional derivatives, fractional differential equations, to methods of their solution and some of their applications, Math. Sci. Eng., 198 (1999). 2
- [21] N. Rai, S. Mondal, Spectral methods to solve nonlinear problems: A review, Partial Differ. Equ. Appl. Math., 4 (2021), 12 pages.
- [22] M. A. Z. Raja, J. A. Khan, I. M. Qureshi, Solution of fractional order system of Bagley-Torvik equation using evolutionary computational intelligence, Math. Probl. Eng., 2011 (2011), 18 pages. 6.1

- [23] M. A. Z. Raja, J. A. Khan, I. M. Qureshi, Swarm intelligence optimized neural networks in solving fractional system of Bagley-Torvik equation, Eng. Intell. Syst., 19 (2011), 41–51.
- [24] M. A. Z. Raja, R. Samar, M. A. Manzar, S. M. Shah, Design of unsupervised fractional neural network model optimized with interior point algorithm for solving Bagley-Torvik equation, Math. Comput. Simul., 132 (2017), 139–158. 6.1
- [25] M. A. Ramadan, A. R. Hadhoud, M. R. Ali, Numerical solutions of singular initial value problems in second-order ordinary differential equations using hybrid orthonormal Bernstein and block-pulse functions, J. Egypt. Math. Soc., 26 (2018), 156–166. 3
- [26] S. S. Ray, A. Atangana, S. C. Noutchie, M. Kurulay, N. Bildik, A. Kilicman, Fractional calculus and its applications in applied mathematics and other sciences, Math. Probl. Eng., 2014 (2014), 2 pages. 1
- [27] A. Saadatmandi, M. Dehghan, A new operational matrix for solving fractional-order differential equations, Comput. Math. Appl., 59 (2010), 1326–1336. 1, 6.1
- [28] S. G. Samko, A. A. Kilbas, O. I. Marichev, Fractional integrals and derivatives: Theory and applications, Gordon and Breach Science Publishers, Yverdon, (1993). 2
- [29] H. Sun, Y. Zhang, D. Baleanu, W. Chen, Y. Chen, A new collection of real world applications of fractional calculus in science and engineering, Commun. Nonlinear Sci. Numer. Simul., 64 (2018), 213–231. 1
- [30] G. Szegö, Orthogonal Polynomials, American Mathematical Society, New York, (1939). 3
- [31] I. Talib, M. Bohner, Numerical study of generalized modified Caputo fractional differential equations, Int. J. Comput. Math., 100 (2023), 153–176. 1
- [32] A. M. Vargas, Finite difference method for solving fractional differential equations at irregular meshes, Math. Comput. Simul., 193 (2022), 204–216.